

4

FILE COPY

AD-A211 687

NUSC Technical Report 6734
1 November 1988

Doppler Statistics of Ocean Velocity Variability

L. Goodman
A. Jilling

Weapon Systems Technology and Assessment Department



DTIC
ELECTE
AUG 24 1989
S B D

Naval Underwater Systems Center
Newport, Rhode Island / New London, Connecticut

Approved for public release; distribution is unlimited.

89 8 24 069

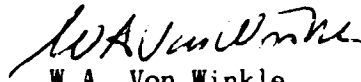
PREFACE

This study was conducted under the Naval Underwater Systems Center's Independent Research/Independent Exploratory Development (IR/IED) Program.

The technical reviewer for this report was K.A. Kemp (Code 8213).

The authors would like to thank the NUSC IR/IED Program Office for its funding support. Also, the authors gratefully acknowledge the reviews and comments offered by K.A. Kemp and P.R. Temple (Code 8219).

REVIEWED AND APPROVED: 1 NOVEMBER 1988



W.A. Von Winkle
Associate Technical Director,
Research and Technology

REPORT DOCUMENTATION PAGE

1a REPORT SECURITY CLASSIFICATION UNCLASSIFIED		1b. RESTRICTIVE MARKINGS	
2a SECURITY CLASSIFICATION AUTHORITY		3 DISTRIBUTION / AVAILABILITY OF REPORT Approved for public release; distribution is unlimited.	
2b DECLASSIFICATION / DOWNGRADING SCHEDULE		5. MONITORING ORGANIZATION REPORT NUMBER(S)	
4 PERFORMING ORGANIZATION REPORT NUMBER(S) TR 6734		7a. NAME OF MONITORING ORGANIZATION	
6a. NAME OF PERFORMING ORGANIZATION Naval Underwater Systems Ctr	6b OFFICE SYMBOL (if applicable) Code 8212	7b. ADDRESS (City, State, and ZIP Code)	
6c ADDRESS (City, State, and ZIP Code) Newport Laboratory Newport, Rhode Island 02841-5047		9. PROCUREMENT INSTRUMENT IDENTIFICATION NUMBER	
8a. NAME OF FUNDING / SPONSORING ORGANIZATION	8b OFFICE SYMBOL (if applicable)	10 SOURCE OF FUNDING NUMBERS	
8c ADDRESS (City, State, and ZIP Code)		PROGRAM ELEMENT NO.	PROJECT NO.
		TASK NO.	WORK UNIT ACCESSION NO.
11 TITLE (Include Security Classification) DOPPLER STATISTICS OF OCEAN VELOCITY VARIABILITY			
12 PERSONAL AUTHOR(S) Goodman, L., and Jilling, A.			
13a TYPE OF REPORT	13b TIME COVERED FROM TO	14 DATE OF REPORT (Year, Month, Day) 88-11-01	15 PAGE COUNT 45
16 SUPPLEMENTARY NOTATION			
17 COSATI CODES		18. SUBJECT TERMS (Continue on reverse if necessary and identify by block number)	
FIELD	GROUP	Underwater Acoustics.	
		Doppler Sonar	
		Ocean Velocity Measurements	
19 ABSTRACT (Continue on reverse if necessary and identify by block number)			
<p>This report examines the returned acoustic signal fluctuations from the backscattering of particles embedded in a model ocean velocity microstructure field. Particular attention is given to the separate role of scatterer relative location. It is shown that the fourth-order statistic of the returned signal or, equivalently, the variance of the pulse-to-pulse returned complex signal correlation function contains information on the spatial structure of the fluid velocity correlation function. A key parameter in this relationship is the ratio of the spatial scale of the fluid velocity field to the along-range scale size of the scattering volume. A sensitivity analysis is performed on the theoretical results comparing the limits of performance of a coherent Doppler estimate of microstructure velocity with those of an estimate involving the use of the higher order statistical relationship, termed stochastic Doppler. Calculations are performed with a typical ocean velocity microstructure field as input</p>			
20 DISTRIBUTION AVAILABILITY OF ABSTRACT <input type="checkbox"/> UNCLASSIFIED/UNLIMITED <input checked="" type="checkbox"/> SAME AS RPT <input type="checkbox"/> DTIC USERS		21 ABSTRACT SECURITY CLASSIFICATION UNCLASSIFIED	
22a NAME OF RESPONSIBLE INDIVIDUAL L. Goodman		22b TELEPHONE (Include Area Code) (401) 841-2051	22c OFFICE SYMBOL Code 8212

19. ABSTRACT (Cont'd)

for a monostatic sonar system operating between 100 kHz and 1 MHz. It is shown that, although coherent Doppler processing does have sufficient sensitivity to resolve typical ocean microstructure velocity, it is severely limited in range capability. On the other hand, the stochastic Doppler technique does have sufficient sensitivity to resolve microstructure velocity with much less restriction on range.



Accession For	
NTIS GRA&I	<input checked="" type="checkbox"/>
DTIC TAB	<input type="checkbox"/>
Unannounced	<input type="checkbox"/>
Justification	
By	
Distribution/	
Availability Codes	
Avail and/or	
Dist	Special
A-1	

TABLE OF CONTENTS

Section		Page
I	INTRODUCTION.....	1
II	SCATTERING MODEL.....	3
III	INPUT OF FLUID VELOCITY STATISTICS.....	12
IV	OCEAN APPLICATION.....	19
V	SUMMARY AND CONCLUSIONS.....	29
VI	BIBLIOGRAPHY.....	31
	APPENDIX -- DERIVATION OF PULSE-TO-PULSE CORRELATION FUNCTION...	A-1

LIST OF ILLUSTRATIONS

Figure		Page
1	Scattering Volume Contribution.....	7
2	Second- and Fourth-Order Moments.....	16
3	Observed Vertical Wavenumber Spectrum of Velocity.....	20

LIST OF TABLES

Table		Page
1a	Sensitivity Limits: Spatial Resolution of Coherent Doppler.....	25
1b	Sensitivity Limits: Spatial Resolution of Stochastic Doppler....	28

DOPPLER STATISTICS OF OCEAN VELOCITY VARIABILITY

I. INTRODUCTION

In the past decade, the oceanographic community has shown a great deal of interest in the use of high-frequency-Doppler sonar to measure the ocean velocity field. Pinkel (1979, 1981) successfully used a 87.5-kHz, 3-kW system mounted on the R/P FLIP to measure the velocity of internal waves. Regier (1982) and Joyce et al. (1982) demonstrated that a Doppler profiler can be employed underway from a ship to measure current shear. L'Hermitte (1973) and Farmer and Crawford (1983) used coherent Doppler sonar techniques to infer ocean currents. Recent review articles in ocean Doppler sonar techniques include Pinkel (1979) and Mathews and Hicks (1981).

Despite all of this recent work in the area of Doppler sonar, there has been only limited research into the relationship between Doppler signal statistics and ocean velocity statistics, and into the intrinsic limits of performance of oceanographic Doppler sonar systems imposed by the nature of the velocity field itself, in particular, by the spatial statistics of the velocity field. Oceanographic Doppler systems typically are limited to estimating the Doppler shift associated with the component of velocity along the mean acoustic ray path of the beam pattern, averaged over the scattering volume. The effect of a random component of the velocity field and the effect of the component of velocity transverse to the mean beam pattern axis is to produce Doppler spectral broadening that is usually treated as noise. (See, for example, Pinkel (1981), who employed the spectral estimation techniques of Rummel (1968) to obtain internal wave-induced Doppler velocities.)

The problem of Doppler broadening by random velocity fluctuations and by flow perpendicular to a finite sized beam pattern has drawn some interest both in the general ultrasound literature (see Mathews and Hicks, 1981) and in the laser flow literature (see Edwards et al., 1971). Doppler broadening by a random velocity field has been considered by a number of authors, including

Green (1964), Rasmussen and Head (1978), Farmer (1983), and L'Hermitte (1983). Their results show that this type of Doppler broadening is proportional to the rms value of the fluctuating velocity.

Brown and Clifford (1973), Brown (1974), and Sullivan and Kemp (1979), among others, examined Doppler broadening effects due the advection of the component of the velocity field perpendicular to the beam pattern axis. Newhouse et al. (1980) and Albright (1976) examined the combination of both of the above effects.

The purpose of this report is to develop a model that will be useful in obtaining the relationship between the space/time statistics of the ocean velocity field and those of the returned acoustic signal for a pulsed, high-frequency, narrowbeam, monostatic sonar system -- the type of system commonly employed in oceanographic measurements. Special attention is given to the statistics of the pulse-to-pulse correlation function, in particular, its variance, which is a fourth-order moment. Also, the utility of using the statistics of the returned signal to infer information about the spatial structure of the microstructure velocity field is analyzed.

II. SCATTERING MODEL

Consider the signal received by a narrowbeam, pulsed, monostatic sonar resulting from the acoustic scattering of discrete particles embedded in a randomly moving fluid. The following assumptions are made:

1. The frequency is sufficiently high that, in the farfield, straightline geometric acoustic propagation applies.
2. The scatterers are assumed to follow the fluid motion perfectly.

The returned signal, then, is a linear sum of reradiated replicas of the transmitted signal, modulated in amplitude by individual particles strength, transmission loss, and the transmitter/receiver beam pattern, and in phase by the location of each scatterer. Only the farfield case will be examined.

A monostatic sonar transmits a series of identical pulses $\phi_T(t)$ of duration T_p repeatable at time interval T_r . Each pulse is expressed as the Fourier series over the pulse duration T_p . Thus,

$$\begin{aligned} \phi_T(t) &= \sum_{k=-\infty}^{\infty} \psi_k \exp(i\omega_k t) && \text{for } -T_p/2 < t < T_p/2, \\ \phi_T(t) &= 0 && \text{for } T_p/2 < t < T_r - T_p/2, \end{aligned} \tag{1a}$$

and

$$\begin{aligned} \phi_T[t - (n - 1)T_r] &= \phi_T(t) && \text{for } 0 \leq t - (n - 1)T_r \leq T_p, \\ &&& n = 1, 2, 3, \dots \end{aligned} \tag{1b}$$

where $\omega_k = 2\pi k/T_p = k\Delta\omega$. The pulse is taken as narrowband about some center frequency ω_q , with

$$|\psi_{q \pm r}| \approx 0,$$

where $r \ll q$, with the bandwidth B given by $B = 2r\Delta\omega$. The contribution of ambiguous scattering volumes in the returned signal is ignored. (This can be accomplished by either taking

$$T_r > 2R_{\max}/c \gg T_p ,$$

where R_{\max} is the maximum range at which the returned scatterer signal is above some prescribed detection threshold, or by the use of a series of narrowband pulses with a sufficiently wide range of center frequencies.)

The returned signal $\phi(t)$ of a narrowbeam, monostatic sonar system operating in the geometric acoustics regime is just the sum of the contributions of the individual discrete scatterers and can be represented by

$$\begin{aligned} \phi(t) &= \int dr b^2(\mathbf{n})\alpha(r)\rho(r,t)\phi_T(t - 2r/c) , \\ &= \int dr \int b^2(\mathbf{n})\alpha(r)\rho(r,t) \sum \psi_k \exp i[\omega_k(t-2r/c)] , \end{aligned} \quad (2)$$

where $b(\mathbf{n})$, $\mathbf{n} = \mathbf{r}/r$ is the beam pattern function. The summation over K will be understood to mean, subsequently, over all k , from $+\infty$ to $-\infty$. The radial integral in equation (2) is also understood to be constrained by the pulse duration, i.e.,

$$c(t - T_p)/2 < r < c(t + T_p)/2 .$$

The discrete scatterer density function $\rho(r,t)$ is defined as

$$\rho(r,t) = \sum_{j=1}^N \delta[r - r(\mathbf{X}_j, t - t_j)] , \quad (3)$$

where $r(\mathbf{X},t)$ is the vector position (at time t) of a fluid element. This representation is termed Lagrangian in fluid dynamics (see Lamb, 1932). The position at initial time $t = 0$, namely \mathbf{X} , is defined by $\mathbf{X} = r(\mathbf{X},0)$. For scatterers being advected with the fluid, \mathbf{X}_j represents the initial position

of the j th scatterer. The factor $t - t_j$ in r of equation (3) is the time at which acoustic energy was reflected from the j th scatterer, which was located at the time of scattering (i.e., $t - t_j$) at location $r(X_j, t - t_j)$.

The discussion is confined to the case where the scatterers follow the fluid perfectly. The quantity $\alpha(r)$ in equation (2) is taken as real and represents the signal amplitude resulting from the combined effects of transmission loss and scattering strength.

Consider the received signal $\phi_m(t)$ due to the m th pulse. From equations (2) and (1b), it follows that

$$\phi_m(t) = \int_V dr \sum \psi_k b^2(n) \alpha(r) \rho(r, t) \exp\{i\omega_k[t - (m-1)T_r - 2r/c]\} . \quad (4)$$

The subscript V in equation (4) indicates that the volume integral is over scatterers ensonified by the m th pulse. A range gate is now applied to $\phi_m(t)$ and the returned gated function $\phi_m(t')$ is defined as

$$\phi_m(t') = h(t') \phi_m(t) , \quad (5)$$

where

$$t' = t - (m - 1)T_r - \tau_m ,$$

and

$$h = h(t') \quad \text{for } -T_I/2 \leq t' \leq T_I/2 ,$$

$$h = 0 \quad \text{otherwise.}$$

Now, take

$$T_I \ll T_r .$$

Here, T_r is the duration of the range gate and τ_m is the time delay of the range gate. Substitution of equation (4) into (5) yields

$$\begin{aligned} \Phi_m(t') &= h(t') \int_V dr \Sigma b^2(\mathbf{n}) \alpha(r) \rho[r, t' + (m-1)T_r + \tau_m] \psi_k \\ &\quad \exp[i\omega_k(t' + \tau_m - 2r/c)] , \\ &\approx h(t') \alpha(R_m) \int_V dr \Sigma b^2(\mathbf{n}) \rho[r, t' + (m-1)T_r + \tau_m] \psi_k \\ &\quad \exp\{i\omega_k[t' + 2(R_m - r)]/c\} , \end{aligned} \quad (6)$$

where $R_m = c\tau_m/2 \gg cT_p/2$. The signal amplitude factor in equation (6) has been taken to be

$$\alpha(r) \approx \alpha(R_m) .$$

The volume integral in (6) at any instant t' (see figure 1) is taken over the range interval

$$r_1 \leq r - R_m \leq r_2 , \quad (7)$$

with

$$r_1 = c(t' - T_p/2)/2 , \quad (8a)$$

and

$$r_2 = c(t' + T_p/2)/2 . \quad (8b)$$

Equation (6) represents the starting point for Doppler processing. Pintel (1981) estimates Doppler shift by calculating an incoherent average of the

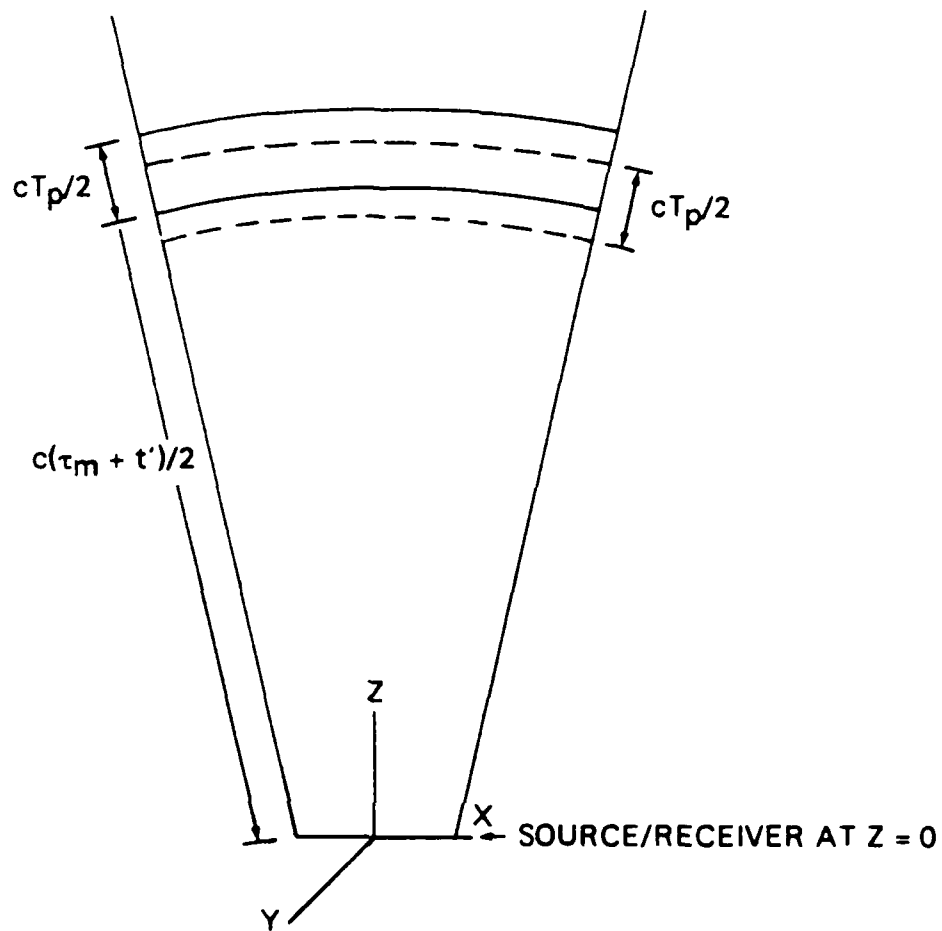


Figure 1. Scattering Volume Contribution

(The radial contribution of scatterers for the m th pulse transmitted during the time interval $(m-1)T_r - T_p/2 \leq t \leq (m-1)T_r + T_p/2$, where T_r is the repetition rate, T_p is the pulse duration, and t' refers to the receiver gate time defined over the gate interval $0 \leq t' \leq T_I - T_p$.)

mean of the spectral estimate of $\Phi_m(t')$ over the gated time interval T_I . (This is a technique first suggested by Rummler, 1968.) The Doppler velocity sensitivity of each estimate in the average is defined by the effective pulse duration and is improved by performing an incoherent average over spectral estimates of a set of pulses over a time period such that the estimated Doppler-shifted velocity remains approximately constant.

In this report, the pulse-to-pulse statistics of $\Phi_m(t')$ will be examined. The statistics of the problem enter through the Lagrangian position vector $r(\mathbf{X}_j, t)$ in the scatterer density function $\rho(r, t)$ given by equation (3). One can decompose $r(\mathbf{X}_j, t)$ as

$$r(\mathbf{X}_j, t) = \mathbf{X}_j + \mathbf{d}_j , \quad (9)$$

where $\mathbf{d}_j = \mathbf{d}(\mathbf{X}_j, t)$ is the relative displacement of a scatterer from its initial position \mathbf{X}_j . Note the difference in the statistics of \mathbf{X}_j and \mathbf{d}_j . \mathbf{X}_j refers to the position of scatterers at a particular instant of time (in this case, the initial instant of time $t = 0$), while \mathbf{d}_j is the displacement from that position due to advection by the fluid velocity field. It will be assumed that \mathbf{X}_j has an equiprobability of initially being anywhere in the spatial domain of the problem (or, equivalently, each of the N scatterers are placed equiprobably throughout the volume). Note that the statistics of \mathbf{X}_j and \mathbf{d}_j are independent and that, therefore, for any function $F(\mathbf{X}_j, \mathbf{d}_j)$, the ensemble average $\langle F(\mathbf{X}_j, \mathbf{d}_j) \rangle$ can be written as

$$\langle F(\mathbf{X}_j, \mathbf{d}_j) \rangle = \langle \langle F \rangle_{\mathbf{X}} \rangle_{\mathbf{d}} = \langle \langle F \rangle_{\mathbf{d}} \rangle_{\mathbf{X}} ,$$

where

$$\langle F \rangle_{\mathbf{X}} = \int d\mathbf{X}_j \, FP(\mathbf{X}_j) ,$$

and

$$\langle F \rangle_{\mathbf{d}} = \int d\mathbf{d}_j \, FP(\mathbf{d}_j) ,$$

respectively, and $P(\)$ indicates the probability density function. The time average is also defined as

$$[(\dots)]_T = (1/T) \int_0^T dt (\dots) ,$$

and the space average as

$$[(\dots)]_L = (1/L) \int_0^L dx (\dots) .$$

It is straightforward to show from equation (6) that the time average of the received signal, the first-order time statistic, is zero:

$$[\phi_m(t')]_{T_I} = 0 . \quad (10)$$

For the second-order statistics, the pulse-to-pulse gated temporal correlation function S'_{nm} is defined in the usual fashion and can be written as

$$S'_{nm} = [\phi_n(t')\phi_m(t')]_{T_I} = \alpha(R_n)\alpha(R_m) \langle h^2(t') \int_{V_n} dr' \int_{V_m} dr'' b^2(n') b^2(n'') \sum_{k,l} \psi_k \psi_l^* \exp\{i(\omega_k - \omega_l)t' + 2i[\omega_l(R_n - r') - \omega_l(R_m - r'')]\}/c \rangle \rho[r', t' + (n-1)T_p + \tau_n] \rho[r'', t' + (m-1)T_p + \tau_m] >_{T_I} , \quad (11)$$

where the scattering volumes V_n, V_m from equation (7) limit the range of integration of (11) to

$$r_1 \leq r' - R_n \leq r_2 ,$$

and

$$r_1 \leq r'' - R_m \leq r_2 ,$$

respectively. Note from equations (8) that $r_1 = c(t' - T_p/2)/2$ and $r_2 = c(t' + T_p/2)/2$. In the appendix, a detailed derivation is carried out for the normalized pulse-to-pulse correlation function $S_{nm} = S'_{nm}/S'_{nn}$ for the case in which the largest scale of the fluctuation field is smaller than the range dimension of the scattering volume. Generalization of these results to the

case where the scattering volume is smaller than the largest scale of the microstructure field, as discussed in the appendix, is straightforward but algebraically complicated. The final result of the appendix derivation is equation (A-31); namely,

$$S_{nm} = \sum_l \psi_l \psi_l^* \int d\mathbf{n}_h b^4(\mathbf{n}_h) \exp[i2\omega_l \bar{v}_h(m-n) T_r \cdot \mathbf{n}_h / c] \\ \exp\{i\omega_l [2\bar{v}_z(m-n) T_r / c - \Delta\tau]\} \int d\xi g(\xi) \exp\{i\omega [2v'_z(m-n) T_r / c]\} , \quad (12)$$

where

$$v'_z = v'_z(z) ,$$

and

$$\xi = (z - R) / \Delta z ,$$

with $\Delta z = cT_p/2$ and $R = R_n$. Also, \bar{v}_z is the mean velocity averaged over the scattering volume, equation (A-26), in the direction of the mean ray axis of the beam pattern; v'_z is the random velocity in the direction of the mean ray axis of the transducer, and v_h is the vector component of velocity perpendicular to the mean ray axis of the beam pattern. The range gate used in deriving equation (12) takes $T_I = T_p$

and

$$h = 1 \quad \text{for } -T_I/2 \leq t' \leq T_I/2 ,$$

$$h = 0 \quad \text{otherwise.}$$

It should be noted that equation (12) has appeared in a variety of forms in the scientific literature. See, for example, Green (1964), Edwards et al. (1971), Albright (1976), and Farmer (1983).

Equation (12) is further simplified by writing it in the form of the product of three terms, namely,

$$S_{nm} = \Sigma \Xi_l K_l Q_l , \quad (13)$$

where

$$\Xi_l = \psi_l \psi_l^* \quad (14)$$

(with Ξ_l normalized, namely, $\Sigma \Xi_l = 1$) is the l th spectral component of the transmitted pulse; and where

$$K_l = \int d\mathbf{n}_h b^4(\mathbf{n}_h) \exp[i2\omega_l \bar{v}_h(m-n)T_r \cdot \mathbf{n}_h/c] \quad (15)$$

represents the contribution from the component of velocity perpendicular to the mean ray axis; and

$$Q_l = \exp[i2\omega_l(m-n)T_r(\bar{v}_z - c\Delta\tau/2)/c] \int d\xi g(\xi) \exp[i2\omega_l(m-n)T_r v'_z/c] \quad (16)$$

is the contribution to the correlation function from the component of velocity along the mean ray axis of the transducer, including both mean and random components. Note that, if $v'_z = 0$ and $v_h = 0$, substitution of equation (16) into (13) yields

$$S_{nm} = \Sigma \psi_l \psi_l^* Q_l = \Sigma \psi_l \psi_l^* \exp\{i \exp[i2\omega_l(m-n)T_r(\bar{v}_z - c\Delta\tau/2)/c]\} . \quad (17)$$

Equation (17) is the theoretical basis for a coherent Doppler estimate of \bar{v}_z .

III. INPUT OF FLUID VELOCITY STATISTICS

Consider the role of the mean along-beam velocity component. From the form of equations (13) and (16), S_{nm} has a maximum if

$$\Delta\tau = 2\bar{v}_z(m - n)T_r/c , \quad (18)$$

which can be interpreted as an along-beam alignment of the m th and n th scattering volumes, which are separated by the time interval $(m - n)T_r$. Equivalently, the phase difference of the two received signals produced by \bar{v}_z in equation (16) can be compensated for by adjusting $\Delta\tau$ to maximize S_{nm} . The use of equation (18) represents a coherent Doppler estimate of the mean velocity in the direction of the sonar axis (L'Hermitte, 1983). The use of equation (18) in (16) results in

$$Q_1 = \int d\xi g(\xi) \exp[i2\omega_1(m-n)T_r v'_z/c] . \quad (19)$$

Consider the factor K_1 in equation (13), which from equation (A-10) is recognized as a fourfold convolution integral of the aperture function w :

$$K_1 = w[\bar{v}_h(m - n)T_r - \mathbf{x}'] * w * w * w , \quad (20)$$

where the convolution operator is defined as

$$U(\mathbf{x} - \mathbf{x}') * V = \int d\mathbf{x} U(\mathbf{x} - \mathbf{x}') V(\mathbf{x}') .$$

It is straightforward to show that if the weight w has characteristic lengths L_x, L_y , then the fourfold convolution of w , i.e., equation (20), also has characteristic lengths L_x, L_y . Thus K_1 , which is the sole contributor to the pulse-to-pulse correlation function in the absence of any radial velocity fluctuations on the scale of the scattering volume and smaller, has a characteristic length scale of the dimensions of the sonar aperture. Therefore, K_1 (and, hence, S_{nm}) becomes small when

$$\bar{v}_h(m - n)T_r > L , \quad (21)$$

where $L = (L_x, L_y)$ is the characteristic vector length scale of the sonar aperture. Thus, \bar{v}_h, L can be combined to form a characteristic time of decorrelation.

Note from equation (19) that Q_1 is a spatial average. Consider the circumstances under which this spatial average can be used in place of an ensemble average over displacement statistics, i.e., when

$$Q_1 = \langle Q_1 \rangle_d . \quad (22)$$

Assuming Gaussian statistics and a homogeneous turbulence (Hinze, 1959) model for the microstructure velocity field yields from equation (19)

$$\langle Q_1 \rangle_d = \int d\xi g(\xi) \langle \exp[i2\omega_1(m-n)T_r v'_z/c] \rangle_d = \exp -\tilde{\tau}^2 , \quad (23)$$

where

$$\tilde{\tau} = (m - n)T_r/\tau_0 , \quad (24a)$$

with

$$(\tau_0)^{-2} = 2\kappa_1^2 \langle (v'_z)^2 \rangle_d , \quad (24b)$$

where $\kappa_1 = \omega_1/c$. Note that τ_0 represents the characteristic decorrelation time associated with v'_z -- the radial velocity fluctuations on the scale of the scattering volume and smaller. It should be noted that results similar to equation (23) have been derived by a number of authors; see, among others, Green (1964), Edwards et al. (1971), Albright (1976), and Farmer (1983).

To examine the validity of equating the spatial average with the ensemble average, i.e., equation (22), consider the variance of Q_1 defined by

$$\begin{aligned} \theta &= \langle (Q_1 - \langle Q_1 \rangle_d)^2 \rangle_d \\ &= \langle Q_1 \rangle_d^2 \iint d\xi d\xi' g(\xi)g(\xi') \{ \exp[2\tilde{\tau}^2 R_v(z-z')] - 1 \} , \end{aligned} \quad (25)$$

where ξ is defined in equation (12) and R_v is the normalized fluctuating z-component velocity correlation function:

$$R_v(z - z') = \langle v'_z(z)v'_z(z') \rangle_d / \langle (v'_z)^2 \rangle_d . \quad (26)$$

The spatial dependence of R_v on the difference variable $z - z'$ results from the assumption of homogeneity for the fluctuating field v'_z . Note that Θ , equation (25), is a fourth-order statistic of the received signal.

By definition, $|R_v| \leq 1$, with the limiting value $R_v = 0$ corresponding to uncorrelated variability on the scale of the scattering volume and smaller for which case, from equation (25), $\Theta = 0$ and

$$Q = \langle Q \rangle_d .$$

However, in general, $R_v \neq 0$ and, thus, $\Theta \neq 0$, and $Q \neq \langle Q \rangle_d$.

As a simple example illustrating the nature of equation (25), set $g(\xi) = 1$ (even though this is not true and g is given by the triangle function, the difference in results being a constant on the order of 1) and let R_v be given by the simple expression

$$\begin{aligned} R_v(z) &= 1 - z/l && \text{for } z \leq l , \\ R_v(z) &= 0 && \text{for } z > l , \end{aligned} \quad (27)$$

where l is interpreted as the characteristic scale of the variability. This simplification still retains the essential physics of the velocity correlation function and its role in equation (25). The resulting Θ is plotted in figure 2 versus $\tilde{\tau}$ for different values of the nondimensional parameter $x_0 = (l/\Delta z)$, the ratio of the velocity variability length scale to the along-range dimension of the scattering volume. Figure 2 also shows a plot of $[\langle Q \rangle_d]^2 =$ fluid velocity field in the z-direction becomes very small compared with the $\exp -2\tilde{\tau}^2$ versus $\tilde{\tau}$. Note that as $x_0 \rightarrow 0$, i.e., the spatial length scale of the

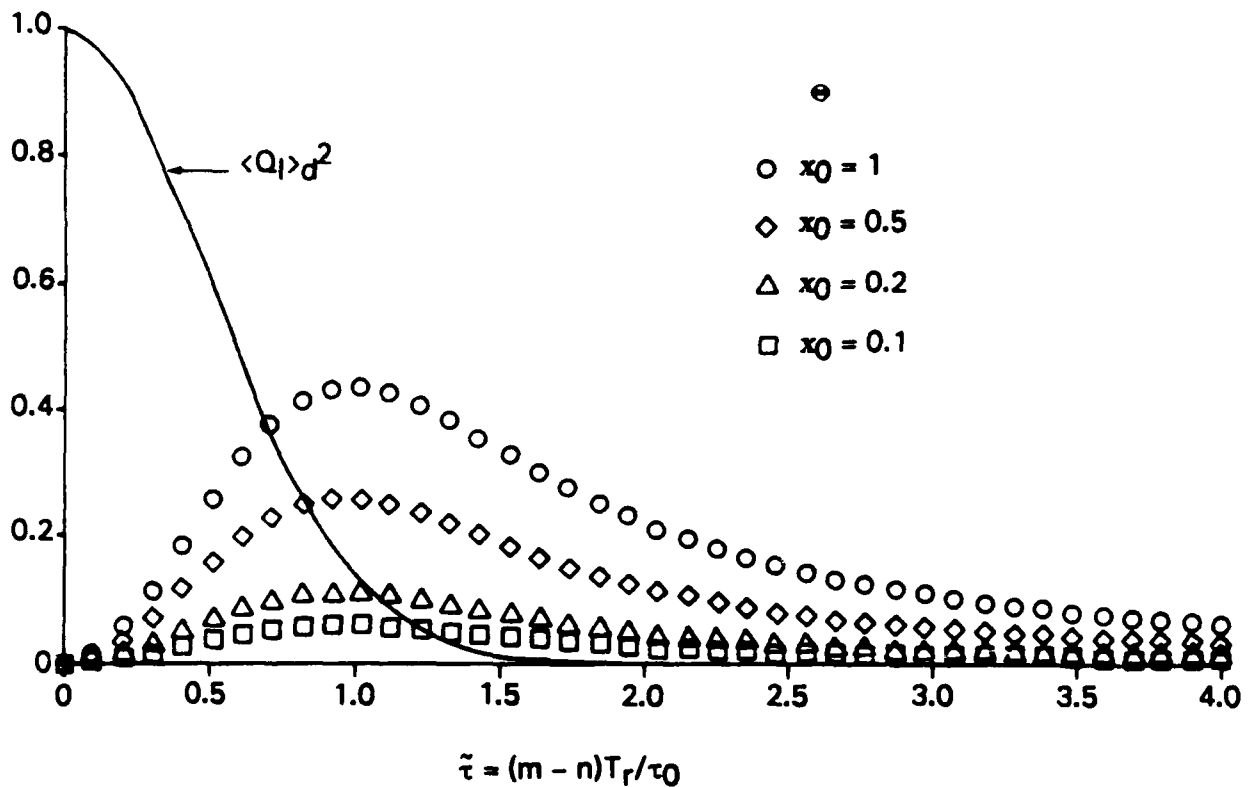


Figure 2. Second- and Fourth-Order Moments
 (The solid line is the function $\langle Q_1 \rangle_d$, equation (23); the symbols refer to families of θ , equation (25), for different ratios of $x_0 = l/\Delta z$, with $g(\xi) = 1$ and equation (27) as the model for microstructure correlation function.)

scattering volume dimension Δz , $\theta \rightarrow 0$. This implies that the variability characterized by scales that are small relative to the scattering volume (in the z -direction) result in small θ and, hence, $Q \approx \langle Q \rangle_d$. As $x_0 \rightarrow 1$, θ increases and $Q \neq \langle Q \rangle_d$. From the general form of equation (25), note that different spatial scales of the velocity field contribute to θ for different $\tilde{\tau}$, the largest scales contributing relatively more for small $\tilde{\tau}$ and the smallest scales contributing more for larger $\tilde{\tau}$. To understand this, note that from equation (25)

$$[d\theta/d(\tilde{\tau}^2)]_{\tilde{\tau}=0} = 2\lambda , \quad (28)$$

where λ is the integral scale defined by

$$\lambda = \iint d\xi d\xi' g(\xi)g(\xi')R_V(z - z') .$$

The integral scale is a measure of the largest scale of the variability. (See Hinze (1959) for a discussion of integral scale in turbulence theory.) This behavior is indicated through the family of different x_0 values in figure 2 by noting the large change in the slope of θ near $\tilde{\tau} = 0$, for increasing x_0 .

At large times $\tilde{\tau}$, only the smallest values of $R_V(z - z')$ (and, hence, smallest scales) contribute, since R_V is, in general, a monotonically decreasing function for realistic ocean microstructure fields. Using the lowest order expansion of $R_V(z - z')$, namely,

$$R_V(z - z') = 1 - |z - z'|^2/(2l_v^2),$$

where l_v is termed the turbulent microscale, which is a measure of the smallest scale of the variability field (see Hinze, 1959, or Tatarski, 1971), in equation (25) yields for $\tilde{\tau} > 1$ the approximation

$$\langle(Q_1)^2\rangle_d = \iint d\xi d\xi' g(\xi)g(\xi') \exp[-(z-z')^2\tilde{\tau}^2/l_v^2] \approx l_v/(\tilde{\tau}\Delta z) . \quad (29)$$

Note that while the function Q_1 contains information on the variance of the velocity field, θ or $\langle(Q_1)^2\rangle_d$ contains additional information on the spatial structure of the velocity field. Conversely, estimates of both Q_1 and θ from measurements might allow estimates not only of the variance $\langle(v'_z)^2\rangle_d$ but also of the velocity correlation function R_V and, in turn, its Fourier transform, the velocity wavenumber spectrum.

IV. OCEAN APPLICATION

The theory developed in sections II and III is applied here to the case of ocean velocity statistics modeled as microstructure. The notation and coordinate system of the earlier sections are continued. Note that the z -coordinate is along the mean ray axis of the beam pattern. The dominant velocity field transverse to the beam axis is in the horizontal. As a concrete example, consider a moored, pulsed, monostatic, sonar system. A comparison will be made between the operational parameters for a Doppler velocity estimate and a velocity estimate that would be inferred through the use of the higher order statistic $\langle(Q_1)^2\rangle_d$, given through equation (25), along with the second-order statistic $\langle Q_1\rangle_d$, from equation (23). This latter estimation technique is called stochastic Doppler because it involves the direct relationship between the ensemble statistics of the acoustic field and the ensemble statistics of the oceanographic velocity field, in contrast to traditional Doppler, which estimates velocity in real time.

The inverse relationship between the statistics of the velocity field and θ or $\langle(Q_1)^2\rangle_d$ is not developed in this section, but is left for a subsequent report. Rather, the limits of performance of the both traditional Doppler and this new stochastic Doppler are examined in terms of the minimum spatial resolution, maximum velocity sensitivity, and ranges potentially achievable, given system noise and the variance of an estimate caused by the finite number of degrees of freedom intrinsic to the measurement of microstructure.

In examining the constraints imposed on real-world operation, other factors will be ignored for simplicity. These include the individual scatterer strength and intrinsic phase variability (apart from relative location, which is considered in this work), scatterer motion relative to the fluid, and phase fluctuations from propagation through random index-of-refraction variability. (Note that it may be possible to infer scatterer motion relative to the fluid to the resolution/sensitivity discussed below if such motion is statistically different from the fluid motion.) In addition, the reader is reminded that an incoherent scatterer model has been used with a large number of scatterers per unit scattering volume.

Small-scale ocean variability, which includes internal waves, finestructure, and microstructure, is here defined as variability on the order of and less than internal waves, i.e., spatial scales of tens of kilometers horizontally, hundreds of meters vertically, time scales between the inertial period (on the order of 24 hours at mid-latitude) and the buoyancy period (typically 10 to 20 minutes). A "canonical" vertical wavenumber spectrum of velocity variability, based on observed data, is shown in figure 3 from Gargett et al. (1981). Note the regimes of internal waves, finestructure, and microstructure. Implicit in this model is that microstructure is isotropic with a characteristic (largest) scale size l , and a dissipative (or smallest) scale size l_v . Note that $l \approx$ meters and $l_v \approx$ centimeters for ocean microstructure and that the spectral level of velocity microstructure varies, following the three curves (I, II, III) of figure 3.

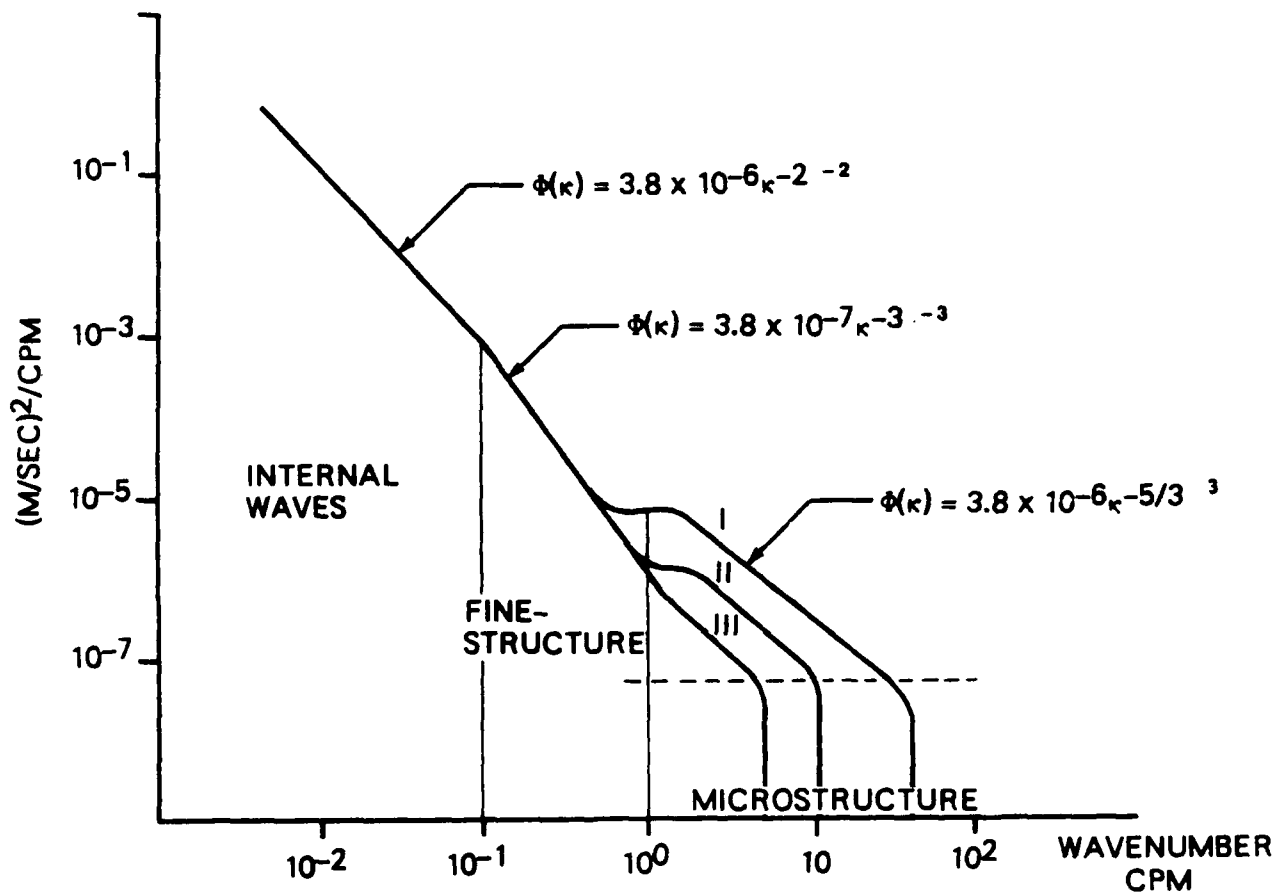


Figure 3. Observed Vertical Wavenumber Spectrum of Small-Scale Ocean Velocity (From Gargett et al. (1981). Shown are three levels of microstructure, labeled I, II, and III. Also indicated are regimes of internal waves, finestructure, and microstructure.)

The Doppler approach is considered first. This analysis is similar to that of Pinkel (1981) for the internal wave range used in the R/P FLIP's 87.5-kHz sonar system, except that the coherent Doppler technique is used (rather than the Rummler (1968) technique), since the problem has been formulated in that manner. It can be shown that the two techniques yield the same level of sensitivity/precision for the same number of independent, real-time, velocity estimates.

The estimate of Doppler velocity is obtained from equation (18) via the shifted time delay $\Delta\tau = 2\bar{v}_z(m - n)T_r/c$, where \bar{v}_z is the spatially averaged mean, defined by equation (A-26) in the appendix. Using equation (17) for the case where v'_z is negligible, which would occur if the scattering volume were sufficiently small, then from equation (16) $Q_1 = 1$ when $\Delta\tau = 2\bar{v}_z(m - n)T_r/c$. However, the contribution of K_1 in equation (13), which contains the effect of motion perpendicular to the mean beam axis and represents a Doppler spread effect, must be considered. (For examination of this effect, see (among others) Green, 1964, and Brown, 1973.) As discussed in section III, K_1 is nonzero over a time scale L/v^* , where v^* is the characteristic velocity of flow perpendicular to the mean beam axis, and L is the characteristic dimension of the sonar in the direction of v^* . Note also that if a mean shear, $q = |\nabla_h v_z|$, of the along-beam velocity is present, it is straightforward to show that there is a decorrelation effect of the same form as equation (20) for the transverse component of flow. The same scaling for a characteristic decorrelation time occurs; namely, L/v^* , with $v^* \approx qR$, R being the range. This can also be derived from equation (A-25) using (A-10) by including the shear term in the expansion for the mean velocity in equation (A-26), whence, with this substitution, the shear term q has the same effect as the mean component of flow perpendicular to the mean ray axis.

Thus, for an estimate of velocity from the pulse-to-pulse correlation function S_{nm} , the time delay between pulses must be restricted to

$$\tau = (m - n)T_r < \tau_{\max} = L/v^* , \quad (30)$$

where v^* is taken as the maximum of qR and the transverse velocity component

(perpendicular to the mean ray axis), and where equation (17) can be used to estimate the Doppler time delay $\Delta\tau$. Note from equation (30) that the maximum number of correlated sequential pulses p is given by

$$p = (m - n)_{\max} = L/(T_r v^*) .$$

The maximum time delay $\Delta\tau = \Delta\tau_{\max}$ over which an estimate of the mean velocity \bar{v}_z can be made is on the order of

$$\Delta\tau_{\max} = 2\bar{v}_z p T_r / c \approx 2L(\bar{v}_z / v^*) / c . \quad (31)$$

To resolve this time shift, which is estimated by maximizing S_{nm} (and hence Q_1) given by equation (16), namely,

$$Q_1 = \exp[i2\omega_1(m-n)T_r(\bar{v}_z - c\Delta\tau/2)/c] ,$$

it is necessary that the fluctuation level of S_{nm} , ΔS , due both to statistical variability of the returned signal (so-called "speckle noise") and system noise, be less than the variation in S_{nm} due to some prescribed variation (desired precision) in \bar{v}_z , $\delta\bar{v}_z$; i.e.,

$$(\Delta S)^2 < 2S_{nm}\delta S = 2S_{nm}(\partial S/\partial\bar{v}_z)_{\max}\delta\bar{v}_z \approx 4\kappa_q L\delta\bar{v}_z/v^* , \quad (32)$$

where the subscript q refers to the center frequency of the transmitted (narrowband) pulse. Equation (32) has been evaluated at τ_{\max} and S_{nm} has been taken as ≈ 1 . If N^{-1} is the system signal-to-noise ratio, then $(\Delta S)^2$ is given by

$$\langle(\Delta S)^2\rangle \approx 2[N^2 + (1/BT_p)] , \quad (33)$$

the factor 2 arising because S_{nm} is a second-order statistic, whence equation (32) becomes

$$[(1/BT_p) + N^2] \leq [2\kappa_q L(\delta\bar{v}_z/v^*)] . \quad (34)$$

Equation (34) can be further simplified. Let l be the spatial scale of the velocity field necessary to be resolved. A pulse duration time T_p must then be chosen that is no longer than

$$T_p = 2 l/c . \quad (35)$$

For a narrow-bandwidth pulse, one can write

$$B \cong \omega_q/Q , \quad (36)$$

where ω_q is the center frequency of the transmitted pulse; for a narrow-beamwidth planar transducer, one can use the approximation (Kinsler et al., 1982)

$$L/(2\pi) = 1/\kappa_q v , \quad (37)$$

where v is the half-angle beamwidth, $\kappa_q = \omega_q/c$. Substituting equations (35) through (37) into (32) yields

$$[Q/(2\kappa_q l) + N^2] \cong [4\pi \delta \bar{v}_z / (v v^*)] . \quad (38)$$

Equation (38) can be considered the fundamental equation for setting sensitivity/resolution limits for the mean Doppler estimate \bar{v}_z .

From figure 3, the model wavenumber spectrum of velocity microstructure goes as $E\kappa^{-5/3}$. The velocity sensitivity $\Delta \bar{v}_z$ corresponding to the spatial scale is given by

$$\delta v_z \cong E' l^{1/3} , \quad (39)$$

where, from figure 3, E' has the typical range of values

$$3 \times 10^{-3} m^{2/3}/sec > E' > 10^{-3} m^{2/3}/sec ,$$

corresponding to strong and weak turbulence limits (i.e., curves I and III.

respectively, in figure 3). Substitution of equation (39) into (38) for the case of zero system noise ($N = 0$) yields the minimum resolution criterion

$$l \geq [Q\upsilon v^*/(8\pi\kappa_q E')]^{0.75} , \quad (40)$$

while for the case dominated by system noise, it yields

$$l \geq [N2\upsilon v^*/(4\pi E')]^3 . \quad (41)$$

As an example, for the sonar parameters,

$$\upsilon = 1^\circ = 1.7 \times 10^{-2} \text{ radians,}$$

$$Q = 15, \text{ and}$$

$$f_0 = 100 \text{ kHz and } 1 \text{ MHz,}$$

table 1a shows the minimum spatial resolution for a signal-to-noise ratio of $20 \log(N) = -10$ dB. A value of $v^* = 0.3$ meter/second and the weak turbulence limit of figure 3 ($E' = 10^{-3} m^{2/3} |^{1/3}$) have been used. Table 1a indicates that over this frequency range coherent Doppler does have sufficient spatial resolution to resolve the microstructure spectrum to scales on the order of centimeters. However, to achieve this resolution for an isotropic microstructure field, the transverse dimension of the scattering volume (perpendicular to the mean ray axis) must be on the order of l and, hence, the range is restricted to

$$R < l/(2\upsilon) \approx 30 l ,$$

with the range limited to less than 1 meter for l on the order of centimeters. However, the range extent of the nearfield of a planar transducer can be written (Kinsler et al., 1982) as

$$R_{\text{nearfield}} = \pi/(8\kappa_q \upsilon^2) \approx 3.25 \text{ meters and } 0.325 \text{ meters}$$

Table 1a. Sensitivity Limits: Spatial Resolution of Coherent Doppler

	$N^2 = 0$	$N^2 = 0.1$
1 MHz	0.44 cm	0.60 cm
100 kHz	2.5 cm	3.1 cm

for the 100-kHz and 1-MHz cases, respectively. Thus, although the sonar has the spatial resolution and velocity sensitivity necessary to resolve microstructure using a coherent Doppler estimate, the range over which this occurs is very restrictive. The upper limit of 1 MHz for the calculation used here was chosen somewhat arbitrarily based on transducer size, power output, and range constraints. However, both equations (40) and (41) show a less than linear increase in spatial resolution with increasing frequency.

Note that equations (23) and (25) establish relationships between the statistics of the received signal and those of the velocity field, namely, $\langle (v'_z)^2 \rangle_d$ and $2[1 - R_V(z)]\langle (v'_z)^2 \rangle_d$, the variance and the structure function, averaged over the scattering volume. Since this average is taken over a spatial scale on the order of the largest scale of the microstructure field, these relationships allow a relaxation of the spatial resolution criteria used in Doppler estimates of the instantaneous velocity fluctuation from the smallest scale of the variability field to the largest scale of the variability, provided that the sensitivity of the estimate of the velocity field statistics is sufficient to resolve the microstructure. This, in turn, would increase the range capability to the order of 30 meters for $l = 1$ meter and to 300 meters for $l = 10$ meters. The estimates of $\langle (v'_z)^2 \rangle_d$ and $2[1 - R_V(z)]\langle (v'_z)^2 \rangle_d$ obtained through the use of equations (23) and (25) are called stochastic Doppler estimates.

From this viewpoint, the sonar parameters are set such that the scattering volume is on the order of (or larger than) the characteristic volume of the velocity microstructure, which is on the order of meters. Note that, for $l > 1$ meter, the mean velocity component \bar{v}_z corresponds to oceanographic processes of larger scale than microstructure and, from equation (38), can be estimated to be on the order of 0.1 mm/sec for $N^2 = 0.1$ and for the same sonar parameters used in the calculations of table 1a. Thus, the variance of a \bar{v}_z estimate corresponding to spatial scales greater than 1 meter would not be a limiting factor in the estimation of parameters associated with the microstructure field by the use of equations (23) and (25). A characteristic parameter that has arisen in the stochastic Doppler relationships of (23) and (25) is the decorrelation time (namely, τ_0) associated with the variability of scales on the order of the scattering volume and smaller given by equation (24a). The maximum number of correlation times obtainable is limited by the effect of transverse flow past the sonar and, following the discussion above, is easily seen as given by

$$\begin{aligned}\tilde{\tau}_{\max} &= \tau_{\max}/\tau_0 = [2\langle(v'_z)^2\rangle_d]^{1/2}\kappa_Q L/v^* \\ &= (2\pi)[2\langle(v'_z)^2\rangle_d]^{1/2}/(v v^*) \approx 1.74\end{aligned}\quad (42)$$

for the sonar parameters used above, with $v^* = 0.3$ meter/second and $\langle(v'_z)^2\rangle_d$ calculated from equation (39) and the weak turbulence limit. To obtain the precision possible using the stochastic Doppler approach, the variance of Q_Q will be used as the fundamental relationship between the acoustics and the fluid velocity field, with the along-beam mean component removed by equation (18). Accordingly, from equations (23) and (25),

$$\langle Q_Q^2 \rangle_d = \iint d\xi d\xi' g(\xi)g(\xi') \{ \exp[-2\tilde{\tau}^2 R_V(z-z')] - 1 \} ,$$

where $\tilde{\tau} \leq \tilde{\tau}_{\max}$, with $\tilde{\tau}_{\max}$ given by equation (42).

From equation (29) with $l = \Delta Z$ for $\tilde{\tau} \approx \tilde{\tau}_{\max}$,

$$\langle Q_Q^2 \rangle_d \approx 1_V / (\tilde{\tau}_{\max} l) = \{ 1_V v^* v [2\langle(v'_z)^2\rangle_d]^{1/2} / (2\pi l) \} . \quad (43)$$

Thus, equation (43) can be used as the smallest $\langle Q_q^2 \rangle_d$ to be resolved in order to have sufficient sensitivity to resolve the smallest scale of the microstructure l_v . Let $(\Delta S)^2$ be the fluctuation level of $(Q_q)^2$ due to speckle noise and system noise; then, since equation (43) is a fourth-order statistic,

$$(\Delta S)^2 = 4(1/BT_p + N^2) . \quad (44)$$

The sensitivity can be further improved if there exists some number of independent samples of the returned signal n_0 over which v'_z is stationary, in which case $(\Delta S)^2$ would be reduced by $1/n_0$. Thus, the criterion for resolving the smallest scale of microstructure l_v is

$$(1/n_0)(\Delta S)^2 < [l_v/(\tilde{\tau}_{\max} l)]^2 . \quad (45)$$

One can write

$$n_0 = \tau_a/\tau_{\max} = v^* \tau_a/L = \alpha l/L , \quad (46)$$

where $\tau_a = \alpha/v^*$ is the time period over which v'_z is statistically stationary. The parameter α is associated with the degree of anisotropy of the larger scale variability generating the microstructure. If this field has physics similar to that of internal waves, one would expect that α is a ratio of horizontal-to-vertical scale of the larger scale field and that $\alpha \approx N/f \approx 100$, where N is the buoyancy frequency and f is the coriolis frequency. (Note that α can be considered as the ratio of the horizontal extent to the vertical extent of a patch of microstructure.) Substituting equations (30), (35)-(37), (44), and (46) into equation (45) yields

$$l_v \leq \{[N^2 + Q/(2\kappa_q l)][64\pi^3 l \langle (v'_z)^2 \rangle_d] / [\kappa_q \alpha v^3 (v^*)^2]\}^{1/2} . \quad (47)$$

For the same sonar parameters as used for the coherent Doppler case (i.e., $Q = 15$, $v = 1^\circ$, and $v^* = 0.3$) but with $l = 1$ meter, the minimum resolvable l_v for the 1-MHz and 100-kHz cases has been calculated and is shown in table 1b. These results suggest that there is sufficient resolution to obtain l_v , although it is somewhat marginal at 100 kHz for the $N^2 = 0.1$ case. Note that

equation (47) depends only on the square root of α , the degree of anisotropy of the microstructure patch. A factor of 10 reduction in α yields a factor of 3 reduction in sensitivity with acceptable values in all cases except the 100-kHz, $N^2 = 0.1$ case. Also, note that equation (47) shows no dependence on l for the noise-free case -- a rather surprising result. Significant improvement in sensitivity can occur by decreasing the mean transverse current (linear dependence). The value of $v^* = 0.3$ meter/second is an upper limit estimate. Finally, although equation (47) shows an increase in sensitivity with increasing beamwidth, the approximation used in equations (40) and (42) involved $\tau_{\max} > 1$, which from equation (42) shows a decrease in τ_{\max} with increasing beamwidth.

Table 1b. Sensitivity Limits: Spatial Resolution of Stochastic Doppler

	$N^2 = 0$	$N^2 = 0.1$
1 MHz	4.26 cm	1.1 cm
100 kHz	13.0 cm	3.5 cm

V. SUMMARY AND CONCLUSIONS

This report has examined the returned signal statistics associated with acoustic scattering from a large collection of scatterers embedded in a model fluid velocity field appropriate for oceanographic application. The fluid velocity field is three-dimensional and contains a microstructure or "turbulent" component. The underlying acoustic model is quite simple -- a monostatic, planar transducer projects very high frequency sound (>100 kHz) into a very large number of identical scatterers that follow the fluid perfectly. Identical pulses are transmitted at some constant repetition rate T_r and then gated at some delay time corresponding to some prescribed range of interest. The propagation is assumed to be in the geometric acoustics regime and only the farfield case is considered. Ambiguous scattering volumes associated with a repetitive set of transmitted pulse trains are ignored. (This problem is addressable either by restricting the repetition rate T_r to be much greater than the travel time to a range where the reverberation level is below some prescribed amount or by using coded pulses.)

The components of velocity that affect the Doppler statistics of the returned signal are:

1. The velocity component in the direction of the beam pattern axis and on the scale of the scattering volume and larger \bar{v}_z ;
2. The velocity component transverse to the direction of the beam pattern axis;
3. The velocity shear field in the direction of the beam pattern axis;
4. The velocity components in the direction of the beam pattern axis and on the scale of the scattering volume and smaller.

Since these effects have been addressed by many authors but in a variety of contexts, a detailed derivation of the relationship of the returned signal statistics in terms of these velocity components is presented in the

appendix; the derivation can be summarized through equations (13), (15), and (16).

The along-beam velocity on the scale of the scattering volume and larger produces a Doppler shift or, equivalently, a time delay in the pulse-to-pulse correlation function S_{nm} . The transverse component of flow produces Doppler broadening or, equivalently, a decorrelation in S_{nm} . The decorrelation time τ_{max} associated with the transverse component of flow is shown to be on the order of L/v^* , where L is a characteristic dimension of the sonar in the direction of the mean transverse flow velocity v^* . This decorrelation time sets a maximum time over which a moored Doppler sonar can receive coherent information for the model scattering field presented in this work.

Decorrelation effects or, equivalently, Doppler spread effects, caused by velocity variability (microstructure) on scales smaller than the scattering volume show up via the statistics of Q_1 , equation (16), and have a characteristic decorrelation time τ_0 , given by equation (24b). Calculations in section IV, i.e., equation (42), using typical oceanographic values and sonar parameters show that $\tau_{max}/\tau_0 \approx 1.7$, and that this ratio is independent of frequency but dependent on the beamwidth and the ratio of the microstructure velocity to the transverse velocity v^* . These results indicate that there is enough time of coherence to obtain the variance of the velocity microstructure.

In section IV a comparison was made between a coherent Doppler estimate and an estimate based on the statistical relationships, equations (23) and (25), called stochastic Doppler. The coherent Doppler estimate from frequency ranges of 100 kHz to 1 MHz has sufficient sensitivity to resolve the smallest scales of ocean velocity microstructure but is very restrictive in range. On the other hand, over the same frequency range, the stochastic Doppler technique also appears to have the sensitivity to resolve the smallest scales of ocean velocity microstructure with much less restriction on range.

VI. BIBLIOGRAPHY

- Albright, R.J. (1976), "Relationship of Doppler Ultrasonic Scattered Signal Characteristics to Flow and Beam Patterns," Journal of the Acoustical Society of America, vol 59, no.4.
- Brown, E.H. (1974), "Turbulent Spectral Broadening of Backscattered Acoustic Pulses," Journal of the Acoustical Society of America, vol 56, no. 5.
- Brown, E.H., and S.C. Clifford (1973), "Spectral Broadening of an Acoustic Pulse Propagating Through Turbulence," Journal of the Acoustical Society of America, vol 54, no. 1.
- Edwards, R.V., J.C. Angus, and J.W. Dunning, Jr. (1971), "Spectral Analysis of the Signal from the Laser Doppler Flowmeter: Time Independent System," Journal of Applied Physics, vol 24, pp 837-850.
- Farmer, D.M., and G.D.R. Crawford (1983), "Measurements of Acoustic Correlation in the Ocean with a High Frequency Echosounder," Nature, vol 36, no. 580, pp 1-3.
- Flatte, S., R. Dashen, W. Munk, K. Watson, and F. Zachariasen (1979), Sound Transmission Through a Fluctuating Ocean, Cambridge University Press, New York.
- Gargett, A.E., P.J. Hendricks, T.B. Sanford, T.R. Osborn, and A.J. Williams (1981), "A Composite Spectrum of Vertical Shear in the Upper Ocean," Journal of Physical Oceanography, vol 11, pp 1258-1271.
- Green, S. (1964), "Spectral Broadening of Acoustic Reverberation in Doppler-Shift Fluid Flowmeters," Journal of the Acoustical Society of America, vol 36, no. 7.
- Hinze, J.O. (1959), Turbulence, McGraw-Hill, New York.
- Joyce, T., D. Bitterman, Jr., and K.E. Prada (1982), "Shipboard Acoustic Profiling of Upper Ocean Currents," Deep Sea Research, vol 29, no. 7A, pp 903-913
- Kinsler, L.E., A.R. Frey, A.B. Coppens, and J.V. Sanders (1982), Fundamentals of Acoustics, John Wiley and Sons, New York.
- Lamb, H., 1932, Hydrodynamics, Cambridge University Press, London.
- L'Hermitte, R. (1983), "Pulse Coherent Doppler Sonar for the Measurement of Water Current and Turbulence," Proceedings of the Acoustic Profiling Symposium, November 1983, IEEE Current Measurement Tech Committee, NOAA.
- Mathews, T. and R.B. Hicks (1981), "Proceedings of the International Symposium on Acoustic Remote Sensing of the Atmosphere and Oceans," University of Calgary, Alberta, Canada.

- Newhouse, V.L., E.C. Furgason, G.F. Johnson, and D.A. Wolf (1980), "The Dependence of Ultrasound Doppler Bandwidth on Beam Geometry," IEEE Transactions on Sonics and Ultrasonics, vol 27, no. 2.
- Papoulis, A. (1965), Probability, Random Variables, and Stochastic Processes, McGraw-Hill, New York.
- Pinkel, R. (1979), "Acoustic Doppler Techniques," MPL-U-86/76, Marine Physical Laboratory, San Diego, CA.
- Pinkel, R. (1980), "On the Use of Doppler Sonar for Internal Wave Measurements," MPL-U-63/79, Marine Physical Laboratory, San Diego, CA.
- Pinkel, R. (1981), "On the Use of Doppler Sonar for Internal Wave Measurements," Deep Sea Research, vol 28A, no. 3, pp 269-280.
- Rasmussen, R.A., and N.E. Head (1978), "Remote Detection of Turbulence from Observations of Reverberation Spectra," Journal of the Acoustical Society of America, vol 63, no. 1.
- Regier, L.A. (1982), "Mesoscale Current Fields Observed with a Shipboard Acoustic Profiling Current Meter," Journal of Physical Oceanography, vol 12, no. 8, pp 880-886.
- Rummler, W.D. (1968), "Introduction of a New Estimator for Velocity Spectral Parameters," Technical Memo Mm-68-4145-5, Bell Telephone Laboratories, Whippany, NJ.
- Sullivan, E.J., and K.A. Kemp (1979), "The Significance of Beam Pattern Side Lobes in Fluid Flow Measurement," Journal of the Acoustical Society of America, vol 66, no. 5.
- Tatarski, V.I. (1971), "The Effects of Turbulent Atmosphere on Wave Propagation," Israel Program for Scientific Translation, Jerusalem.

APPENDIX
DERIVATION OF PULSE-TO-PULSE CORRELATION FUNCTION

As discussed in the body of this report, the first-order statistics of the received signal $\phi_m(t')$ are zero, as would be expected. For the second-order statistics,

$$\Theta_{nm} = \phi_n \phi_m^* .$$

Then, the pulse-to-pulse gated autocorrelation function, equation (11), is given by

$$S_{nm} = [h^2(t')\Theta_{nm}]T_I , \quad (A-1)$$

with

$$\Theta_{nm} = \alpha(R_n)\alpha(R_m) \int_{V_n} dr' \int_{V_m} dr'' b^2(n')b^2(n'') \sum_{k,l} \psi_k \psi_l^* \exp\{i(\omega_k - \omega_l)t' + 2i[\omega_k(R_n - r') - \omega_l(R_m - r'')]\}/c\} \\ \rho[r', t' + (n-1)T_r + \tau_n] \rho[r'', t' + (m-1)T_r + \tau_m] ,$$

and the scattering volumes V_n and V_m are limited in radial extent by

$$r_1 \leq r' - R_n \leq r_2 \quad \text{for } V_n ,$$

and

$$r_1 \leq r' - R_m \leq r_2 \quad \text{for } V_m ,$$

with

$$r_1 = c(t' - T_p/2)/2 , \quad (A-2a)$$

$$r_2 = c(t' - T_p/2)/2 . \quad (A-2b)$$

Since the initial position of each scatterer X_j is taken as equiprobable, the density function ρ , being a sum of delta functions, can be considered from the definition of the Lagrangian position vector r , i.e., from

$$r(X_j, t) = X_j + d_j ,$$

as a Poisson process with respect to X_j (Albright, 1976). Note, also, that the scatterer displacement is assumed to be small enough that the explicit time dependence in $\rho(r, t)$ can be neglected over the pulse duration time T_p and the range gate time T_I . Since the scatterer initial position X_j can be described by a Poisson process, it is straightforward to show that to order $1/N$, where N is the average number of scatterers in the scattering volume,

$$S_{nm} = [h^2(t')\Theta_{nm}]_{T_I} \approx \langle [h^2(t')\Theta_{nm}]_{T_I} \rangle_X = [h^2(t')\langle \Theta_{nm} \rangle_X]_{T_I} , \quad (A-3)$$

where

$$\begin{aligned} \langle \Theta_{nm} \rangle_X &= \alpha(R_n)\alpha(R_m) \int_{V_n} dr' \int_{V_m} dr'' b^2(n')b^2(n'') \sum_{k,l} \psi_k \psi_l^* \\ &\quad \exp\{i(\omega_k - \omega_l)t' + 2i[\omega_k(R_n - r') - \omega_l(R_m - r'')]\}/c\} \\ &\quad \langle \rho[r', t' + (n-1)T_r + \tau_n] \rho[r'', t' + (m-1)T_r + \tau_m] \rangle_X \\ &= \alpha(R_n)\alpha(R_m) \int_{V_n} dr' \int_{V_m} dr'' b^2(n')b^2(n'') \sum_{k,l} \psi_k \psi_l^* \\ &\quad \exp\{i(\omega_k - \omega_l)t' + 2i[\omega_k(R_n - r') - \omega_l(R_m - r'')]\}/c\} \rho_0 \delta(r' - r'' + s). \end{aligned} \quad (A-4)$$

Note that the second-order statistic for a Poisson process (Papoulis, 1965) has been used; namely,

$$\begin{aligned}
& \langle \rho[\mathbf{r}', t' + (n-1)T_R + \tau_n] \rho[\mathbf{r}'', t' + (m-1)T_R + \tau_m] \rangle_X \\
& \cong \langle \rho[\mathbf{r}', (n-1)T_R + \tau_n] \rho[\mathbf{r}'', (m-1)T_R + \tau_m] \rangle_X \\
& = \rho_0^2 + \rho_0 \delta(\mathbf{r}' - \mathbf{r}'' + \mathbf{s}) , \tag{A-5}
\end{aligned}$$

where

$$\mathbf{s} = \mathbf{d}[X, (m-1)T_R + \tau_m] - \mathbf{d}[X, (n-1)T_R + \tau_n]$$

is the displacement of a fluid element, initially at X , during the time interval between the scattering of the n th and m th pulse. Again, since it has been assumed that the pulse duration T_p and the gate function T_I are kept sufficiently small, the explicit time dependence of ρ on t' can be neglected in equation (A-4). However, since $T_R \gg T_p + T_I$, the dependence on pulse-to-pulse time delay cannot be ignored. Note that the first term on the right-hand side of equation (A-5) does not contribute to (A-4) by virtue of equation (10). (The product of two zero-mean value terms is zero.)

Consider the effect of the delta function on the beam pattern functions of equation (A-4). For nonzero contributions, the delta function in (A-4) requires that

$$\mathbf{r}'' = \mathbf{r}' + \mathbf{s} .$$

Then,

$$\mathbf{n}'' = (\mathbf{r}' + \mathbf{s}) / |\mathbf{r}' + \mathbf{s}| \cong \mathbf{n}' , \tag{A-6}$$

since the displacements of the scatterer over the time intervals between pulses are such that

$$|\mathbf{s}| \ll |\mathbf{r}'| .$$

For the effect of the delta function on the radial spatial variables of

equation (A-4), note that contributions can occur only if the double integral overlaps and, hence, that

$$|r' - r'' + s| \leq cT_p/2 .$$

The condition for overlap of the radial component of the spatial integrals of equation (A-4) can be written

$$R_m = R_n + c\Delta\tau/2 = R + c\Delta\tau/2 , \quad (A-7)$$

where R is now identified as the range to the n th scattering volume, used as a reference. The time delay $\Delta\tau$ will be used to estimate a mean Doppler shift. Integrating over the delta function in equation (A-4) using (A-6) results in

$$\begin{aligned} \langle \Theta_{nm} \rangle_X = R^2 \alpha^2(R) \rho_0 \int_{V_0} dr b^4(\mathbf{n}) \sum_{k,l} \psi_k \psi_l^* \\ \exp\{i(\omega_k - \omega_l)[t' + 2(R-r)/c] - i\omega_l(\Delta\tau - 2S_r/c)\} , \end{aligned} \quad (A-8)$$

where V_0 , the scattering volume, constrains the range interval by

$$r_1 \leq r - R \leq r_2 ,$$

with r_1 , r_2 defined by equations (A-2a) and (A-2b), respectively. The radial displacement S_r is given by

$$S_r = \mathbf{n} \cdot \mathbf{s} . \quad (A-9)$$

Note that in the dummy spatial variable r of integration in equation (A-8) the prime notation has been dropped.

The beam pattern function can be written in the farfield as the Fourier transform of the aperture function $w(\mathbf{x})$; namely,

$$b(\mathbf{n}) = \int d\mathbf{x} w(\mathbf{x}) \exp(i\omega_0 \mathbf{n} \cdot \mathbf{x}/c) , \quad (A-10)$$

where attention is confined to a planar sonar and \mathbf{x} is taken in the x,y plane, i.e., $\mathbf{x} = (x,y,0)$. (Note that the effect of finite frequency bandwidth dependence of the beam pattern has been neglected; this effect can easily be taken into account for the narrowband pulses in the analysis by replacing $b(\mathbf{n})$ with $b_k(\mathbf{n})$, where k indicates the pulse Fourier series component number. The frequency ω_0 is the center frequency of transmission.)

Note that for a planar sonar

$$\mathbf{n} \cdot \mathbf{x} = n_h \cdot \mathbf{x} ,$$

where n_h is the vector component of the radial unit vector \mathbf{n} in the x,y plane, i.e.,

$$n_h = (n_x, n_y, 0) .$$

Then,

$$b(\mathbf{n}) = b(n_h) . \tag{A-11}$$

Substitution of equation (A-11) into (A-8) yields

$$\langle \Theta_{nm} \rangle_X = \frac{R^2 \alpha^2(R) \rho_0}{V_0} \int dr b^4(n_h) \sum_{k,l} \psi_k \psi_l^* \exp\{i(\omega_k - \omega_l)[t' + 2(R-r)/c - i\omega_l(\Delta\tau - 2S_r/c)]\} . \tag{A-12}$$

For a narrowbeam sonar,

$$n_z = \cos(\nu) \approx 1 ,$$

since the polar angle ν , defined with respect to the mean ray axis (taken as the z -direction), is small, i.e., $\nu \ll 1$. Then, the radial spatial variable of integration in equation (A-12) approximates to

$$r \cong r \cos(\nu) = z , \quad (\text{A-13})$$

over the limits given by (A-9):

$$r_1 \cong z - R \cong r_2 , \quad (\text{A-14})$$

where r_1 , r_2 are given by equations (A-2a) and (A-2b), respectively. By definition, the spatial variables of integration of equation (A-12) in the x,y plane can be written as

$$x = r n_h \cong z n_h \quad (\text{A-15})$$

by virtue of (A-13). Using equations (A-13) and (A-15), the spatial volume element of (A-9) can be written as

$$d^3x \cong z^2 dz dn_h \cong R^2 dz dn_h ,$$

which results in (A-12) becoming

$$\langle \Theta_{nm} \rangle_X = R^2 \alpha^2(R) \rho_0 \int dn_h b^4(n_h) \int_{R+c(t'-T_p/2)/2}^{R+c(t'+T_p/2)/2} dz \exp\{i(\omega_k - \omega_l)[t' + 2(R-z)/c] - i\omega_l(\Delta\tau - 2S_r/c)\} . \quad (\text{A-16})$$

Let

$$f_1(z) = \exp(2i\omega_l S_r/c) ,$$

where

$$-cT_p/4 < z - R - ct'/2 < cT_p/4 . \quad (\text{A-17})$$

To simplify equation (A-16), $f_1(z)$ is expanded over (A-17) in the Fourier series

$$f_1(z) = \exp(2i\omega_1 S_r/c) = \sum_j a_{1j} \exp[i(z-R-ct'/2)\kappa_j] , \quad (\text{A-18})$$

where

$$\kappa_j = 2\pi j/(cT_p/2) ,$$

and

$$a_{1j} = 1/(cT_p/2) \int_{R+ct'/2-cT_p/4}^{R+ct'/2+cT_p/4} dz \exp(2i\omega_1 S_r/c) \exp[-i(z-R-ct'/2)\kappa_j] , \quad (\text{A-19})$$

which, upon substitution into equation (A-16) and after some straightforward algebra, yields

$$\begin{aligned} \langle \Theta_{nm} \rangle_X = R^2 \alpha^2(R) \rho_0 \int dn_h b^4(n_h) (cT_p/2) \sum_{l,j} \psi_{l+j} \psi_{l+j}^* \\ \exp(-i\omega_1 \Delta\tau) a_{l,j} , \end{aligned} \quad (\text{A-20})$$

and then substituting equation (A-20) into (A-3) yields

$$\begin{aligned} S_{nm} = R^2 \alpha^2(R) \rho_0 \int dn_h b^4(n_h) (cT_p/2) \sum_{l,j} \psi_{l+j} \psi_{l+j}^* \\ \exp(-i\omega_1 \Delta\tau) [h^2(t') a_{l,j}] T_p . \end{aligned} \quad (\text{A-21})$$

Equation (A-20) shows that, in general, individual Fourier components of the transmitted pulse mix, i.e., $\psi_{l+j} \psi_{l+j}^*$, contribute for $m \neq 0$ to the correlation function S_{nm} . Note that for homogeneous Gaussian displacement statistics,

$$\langle S_r(z') S_r(z'') \rangle_d = F(z'' - z') ,$$

$$\langle a_{l,j} \rangle_d = 0 \quad \text{for } j \neq 0 ;$$

thus, for $\langle S_{nm} \rangle$, no mixing of pulse Fourier components occurs. So, if one chooses a scattering volume sufficiently large to include all the scales of variability, one expects that

$$\{a_{1,j}\}_{T_p} = \langle a_{1,j} \rangle_d = 0 \quad \text{for } j \neq 0 . \quad (\text{A-22})$$

If one assumes condition (A-22) in equation (A-21),

$$S_{nm} = R^2 \alpha^2(R) \rho_0 \int dn_h b^4(n_h) (cT_p/2) \psi_1 \psi_1^* \exp(-i\omega_1 \Delta\tau) [h^2(t') a_{1,0}]_{T_p} . \quad (\text{A-23})$$

It should be noted that it is straightforward to include the $j \neq 0$ terms in equation (A-23) and in the analysis of section III. Note that the last term of (A-23) can be written for $h = 1$ as

$$\begin{aligned} [h^2(t') a_{1,0}]_{T_p} &= (a_{1,0})_{T_p} \int_{-T_p/2}^{T_p/2} h^2 dt' \left[\begin{array}{c} R+ct'/2+cT_p/4 \\ \int dz \exp(2i\omega_1 S_T/c) \\ R+ct'/2-cT_p/4 \end{array} \right] \\ &= \int g(\xi) d\xi \exp[2i\omega_1 S_T(z)/c] , \end{aligned} \quad (\text{A-24})$$

where $g(\xi)$ is the triangle function:

$$\begin{aligned} g(\xi) &= 1 - \xi & \text{for } 0 \leq \xi \leq 1 , \\ &= \xi - 1 & \text{for } -1 \leq \xi \leq 0 , \\ &= 0 & \text{otherwise ,} \end{aligned}$$

and where $\xi = (z - R)/\Delta z$, with $\Delta z = cT_p/2$. Thus,

$$S_{nm} = R^2 \alpha^2 (R) T_p \rho_0 \Sigma \int dn_h b^4(n_h) \psi_l \psi_l^* \int g(\xi) d\xi \exp\{-i\omega_l [\Delta\tau - 2S_r(z)/c]\}. \quad (A-25)$$

The form of equation (A-25) suggests decomposing the displacement field into a mean and fluctuating component as follows

$$s = \bar{s} + s' , \quad (A-26)$$

where the overbar notation is used to indicate the weighted spatial average:

$$\bar{f}(\bar{z}) = \int g(\xi) f(z).$$

Thus, by definition,

$$\begin{aligned} \bar{s} &= \bar{d}[X, (m-1)T_r + \tau_m] - \bar{d}[X, (n-1)T_r + \tau_n] , \\ &= \bar{v}(m-n)T_r , \end{aligned} \quad (A-27)$$

where equation (A-7) has been used and, hence, $\tau_m = \tau_n + \Delta\tau$, $\Delta\tau \ll \tau_n$, $\tau_m < T_r$, and where the time interval $(m-n)T_r$ has been selected to be small enough that the mean velocity \bar{v} does not change significantly over $(m-n)T_r$. The fluctuating displacement s' can be written as

$$s' = d'[X, (m-1)T_r + \tau_m] - d'[X, (n-1)T_r + \tau_n] . \quad (A-28)$$

Note that for turbulence-like fluctuations, if $(m-n)T_r < \tau_\lambda$, where τ_λ is the temporal microscale, the frozen field hypothesis (Hinze, 1959) can be invoked and s' can also be written in the form

$$s' = (m-n)T_r v'(X) , \quad (A-29)$$

where v' is the fluctuating velocity defined analogously to equation (A-27). Substituting equations (A-27) and (A-29), using (A-10), into equation (A-25) yields

$$S_{mn} = R^2 \alpha^2 (R) T_{p\rho 0} \sum_l \psi_l \psi_l^* \int dn_h b^4(n_h) \exp[i2\omega_l \bar{v}_h(m-n) T_r \cdot n_h / c] \\ \exp\{i\omega_l [2\bar{v}_z(m-n) T_r / c - \Delta\tau]\} \int d\xi g(\xi) \exp\{i\omega [2v'_z(m-n) T_r / c]\}, \quad (A-30)$$

where the overbar and prime notation (for mean and fluctuating) have been combined with the vector component notation subscript h (indicating along the x/y plane) and subscript z (indicating the direction of the mean ray axis).

Note that $\bar{s}_h = \bar{v}_h(m-n) T_r \gg s'_h$. (It is straightforward to include the term $s'_h \sim v'_h(m-n) T_r$ with some additional algebra. However, most realistic oceanographic cases will allow this generalization since the oceanographic velocity variability is typically "red" in wavenumber spectra.) To normalize equation (A-30), take S_{nm}/S_{nn} , which amounts to setting

$$R^2 \alpha^2 (R) T_{p\rho 0} = 1,$$

and

$$\sum_l \psi_l \psi_l^* = 1.$$

After redefining S_{nm} as the normalized pulse-to-pulse gated correlation function with $S_{nn} = 1$ from equation (A-30), the above normalization then yields

$$S_{nm} = \sum_l \psi_l \psi_l^* \int dn_h b^4(n_h) \exp[i2\omega_l \bar{v}_h(m-n) T_r \cdot n_h / c] \\ \exp\{i\omega_l [2\bar{v}_z(m-n) T_r / c - \Delta\tau]\} \int d\xi g(\xi) \exp\{i\omega [2v'_z(m-n) T_r / c]\}. \quad (A-31)$$

INITIAL DISTRIBUTION LIST

Addressee	No. of Copies
DTIC	12
CNA	1
CNR (OCNR-00, OCNR-10, OCNR-11, OCNR-12, OCNR-122, OCNR-123, OCNR-13, OCNR-20)	8
ONR Detachment, St. Louis	1
ONR Detachment, Boston	1
ONR Detachment, Pasadena	1
NRL	1
NORDA	1
NPS	1
COMNAVOCEANCOM	1
NOO	1
FLENUMOCEANCEN	1
APL, Johns Hopkins	1
APL, U. of Washington	1
APL, U. of Texas	1